HHS Public Access

Author manuscript

Hypertension. Author manuscript; available in PMC 2019 September 25.

Published in final edited form as:

Hypertension. 2018 September ; 72(3): 632–640. doi:10.1161/HYPERTENSIONAHA.118.10907.

Tumor Cell Subtypes Based on the Intracellular Hormonal Activity in *KCNJ5*-Mutated Aldosterone-Producing Adenoma

Yuto Yamazaki, **Kei Omata**, **Yuta Tezuka**, **Yoshikiyo Ono**, **Ryo Morimoto**, **Yuzu Adachi**, **Kazue Ise**, **Yasuhiro Nakamura**, **Celso E. Gomez-Sanchez**, **Yukiko Shibahara**, **Takumi Kitamoto**, **Tetsuo Nishikawa**, **Sadayoshi Ito**, **Fumitoshi Satoh**, **Hironobu Sasano**

Department of Pathology (Y.Y., K.I., Y.N., H.S.) and Division of Clinical Hypertension, Endocrinology and Metabolism (K.O., Y.T., F.S.), Tohoku University Graduate School of Medicine, Sendai, Japan; Division of Nephrology, Endocrinology, and Vascular Medicine (K.O., Y.T., Y.O., R.M., S.I., F.S.) and Department of Pathology (Y.A.), Tohoku University Hospital, Sendai, Japan; Department of Pathology, University of Michigan Medical School, Ann Arbor (K.O.); Division of Metabolism, Endocrinology and Diabetes, Department of Internal Medicine, University of Michigan, Ann Arbor (Y.O.); Division of Pathology, Faculty of Medicine, Tohoku Medical and Pharmaceutical University, Sendai, Japan (K.I., Y.N.); Division of Endocrinology, Department of Medicine, The University of Mississippi Medical Center, Jackson (C.E.G.-S.); Research and Medicine Services, G.V. (Sonny) Montgomery VA Medical Center, Jackson, MS (C.E.G.-S.); Department of Pathology (Y.S.) and Endocrinology and Diabetes Center (T.K., T.N.), Yokohama Rosai Hospital, Japan; and Division of Endocrinology, Department of Medicine, Columbia University, New York, NY (T.K.).

Abstract

Aldosterone-producing adenomas (APAs) harbor marked intratumoral heterogeneity in terms of morphology, steroidogenesis, and genetics. However, an association of biological significance of morphologically identified tumor cell subtypes and genotypes is virtually unknown. *KCNJ5* mutation is most frequently detected and generally considered a curable phenotype by adrenalectomy. Therefore, to explore the biological significance of *KCNJ5* mutation in APA based on intracellular hormonal activities, 35 consecutively selected APAs (n=18; *KCNJ5* mutated, n=17; wild type) were quantitatively examined in the whole tumor areas by newly developed digital image analysis incorporating their histological and ultrastructural features (14 cells from 2 *KCNJ5*-mutated APAs and 15 cells from 1 wild type) and CYP11B2 immunoreactivity. Results demonstrated that *KCNJ5*-mutated APAs had significantly lower nuclear/cytoplasm ratio and more abundant clear cells than wild type. CYP11B2 immunoreactivity was not significantly different between these genotypes, but a significant correlation was detected between the proportion of clear cells and CYP11B2 immunoreactivity in all of the APAs examined. CYP11B2 was predominantly immunolocalized in clear cells in *KCNJ5*-mutated APAs. Quantitative

Reprint requests to: Hironobu Sasano, Department of Pathology, Tohoku University School of Medicine, 2-1 Seiryo-machi, Aoba-ku, Sendai, 980-8575 Japan. hsasano@patholo2.med.tohoku.ac.jp.

Disclosures

None.

The online-only Data Supplement is available with this article at https://www.ahajournals.org/doi/suppl/10.1161/HYPERTENSIONAHA.118.10907.

ultrastructural analysis revealed that *KCNJ5*-mutated APAs had significantly more abundant and smaller-sized mitochondria with well-developed cristae than wild type, whereas wild type had more abundant lipid droplets per unit area despite the small number of the cases examined. Our results did provide the novel insights into the morphological features of APA based on their biological significance. *KCNJ5*-mutated APAs were characterized by predominance of enlarged lipid-rich clear cells possibly resulting in increased neoplastic aldosterone biosynthesis.

Keywords

adrenocortical adenoma; aldosterone; cytochrome P-450 CYP11B2; hyperaldosteronism; immunohistochemistry; mitochondria; mutation

Primary aldosteronism is a major cause of secondary hypertension, accounting for 5% to 10% of all the patients with hypertension.[1–3] Aldosterone-producing adenoma (APA) is one of the major subtypes of primary aldosteronism. APA has been well known to be associated with marked intratumoral heterogeneity in terms of its morphology and steroidogenesis including CYP11B2 (aldosterone synthase) status.[4,5]

Histologically, APA has been reported to be mainly composed of clear cells and compact cells.[4] Clear cells have been considered as biologically quiescent represented by low CYP11B2 immunoreactivity and tentatively classified as zona fasciculata-like cells based on the similarity of their morphological features.[6–9] On the other hand, compact cells have been considered as biologically active and also classified as zona glomerulosa (ZG)-like cells.[6–9] However, biological and clinical significance of these histologically defined clear and compact cells have not been explored.

Recently, somatic gene mutations associated with autonomous aldosterone oversecretion have been reported within *KCNJ5, ATP1A1, ATP2B3, CACNA1D*, and *CTNNB1*.[10–13] Among those mutations above, *KCNJ5* somatic mutations have been most frequently detected, particularly in ≈70% of Japanese APA patients.[14] *KCNJ5*-mutated APAs have been generally considered curable phenotype by adrenalectomy with the patients harboring the mutant APAs having a higher lateralization ratio during adrenal vein sampling.[15,16] In addition, the relatively close association of individual genotypes with histological characteristics of APA has been previously proposed.[6,7,10] However, these previously reported morphological and immunohistochemical studies were all based on the eyeball estimation.[6,7,10,17] To the best of our knowledge, the detailed intratumoral morphological and biological differences among APAs of these different genotypes based on the quantitative evaluation have not been reported.

Recently, digital image analysis (DIA) based on virtual microscopic examination has been developed and could provide the quantified results with high reproducibility in various diseases.[18–21] Therefore, in this study, detailed morphological features and the status of CYP11B2 immunoreactivity in APAs harboring *KCNJ5* mutation and wild type were quantitatively evaluated by using newly developed DIA system to further explore the biological significance of genotypes in APA and to provide its possible novel histopathological classification.

Materials and Methods

The data that support the findings of this study are available from the corresponding author upon reasonable request.

APA Cases

Thirty-five consecutively available APA cases were retrieved from 2 different institutions in Japan (18 *KCNJ5*-mutated APAs from Tohoku University Hospital from 2010 to 2013 and 17 wild-type APAs from Yokohama Rosai Hospital from 2008 to 2014). These cases were all clinically diagnosed according to the Endocrine Society Guidelines for primary aldosteronism.[1] Blood pressure was measured according to our previous reports in individual institutions.[22,23] All the specimens were histopathologically diagnosed as adrenocortical adenoma based on the criteria of Weiss[24] and also confirmed as APAs based on the results of CYP11B2 immunohistochemistry.[25] The whole tumor area was available in the representative tissue sections to fully evaluate the intratumoral heterogeneity of APA in all the cases examined. The research protocols of this study were approved by each local Institutional Review Board.

RNA Extraction and Aldosterone-Driver Gene Somatic Mutation Analysis by Sequencing

A piece of frozen tissue was obtained from all of these cases, and RNA extraction was performed in individual institutions. For the cases from Tohoku University, Sanger sequencing was performed as we previously reported.[26] Consecutively available 18 cases with *KCNJ5* mutation at G151R or L168R were selected. Somatic mutation status of APA cases from Yokohama Rosai Hospital was examined according to the protocol we previously reported.[17,23] Consecutively available 17 cases without any kinds of known driver mutations, such as *ATP1A1, ATP2B3, CACNA1D*, and *CTNNB1*, were selected.[1723] All the results of the Sanger sequence were referred to the previous reports to confirm the true positive somatic mutation of these targeted genes.[27]

Morphological Evaluation Using DIA

All the resected adrenal specimens were entirely submitted for histo-pathological examination after 10% neutral formalin fixation and paraffin embedding. Hematoxylin and eosin (H&E) sections were made at 3 μm prepared from these formalin fixation and paraffin embedding tissue blocks. All of the H&E-stained tissue sections were made manually by 1 experienced histotechnician at the Department of Pathology, Tohoku Graduate School of Medicine, exactly in the same fashion based on the protocol described in Figure S1 in the online-only Data Supplement. All of the H&E sections were subsequently digitally scanned and captured using Image Scope AT2 (Leica, Wetzlar, Germany) to perform further analysis. They were carefully assessed by the DIA system using the software of HALO Area Quantification ver. 1.0 (Indica Laboratories, Corrales, NM). We proceeded with the following 3 steps and set all the parameters to achieve quantitative morphological evaluation. The series of the DIA steps were summarized in Figure 1. At first, the whole tumor area was initially classified into parenchyme and mesenchyme based on the histological architectural patterns, including the cell shape and color spectrums. Second, parenchyme (parenchymal area) was subsequently classified into nuclear and cytoplasm

based on the color spectrums (nuclear: purple [hematoxylin], cytoplasm: nonpurple). Finally, cytoplasm (the area classified into cytoplasm in the parenchyme) was further classified into clear cells and compact cells based on the gradients of the eosinophilic color spectrum (Figure 1A). The percentage of individual histological components, parenchyme, mesenchyme, nuclear, and cytoplasm, were calculated against the whole tumor area. Those of the proportion of clear cell, compact cell, CYP11B2 positive area, and CYP11B2 *H* score were calculated against the cytoplasm in the parenchyme.

We also evaluated the degrees of paradoxical hyperplasia which is generally detected in the adjacent ZG of APA[28] by calculating the percentage of the occupying area of adjacent ZG in the adjacent adrenal cortex in these H&E sections using the Image-Scope v12.01.5027 (Leica, Aperio, Wetzlar, Germany). In addition, total number of the tumor cells was counted in H&E sections by the software of HALO Cytonuclear ver. 1.5 (Indica Laboratories, Corrales, NM) in the same whole tumor area examined above and calculated the average size of individual tumor cells.

Immunohistochemistry and Evaluation of CYP11B2 Immunoreactivity Using DIA

After carefully reviewing the H&E sections of all the cases above, CYP11B2 immunohistochemistry (hCYP11B2, 1:500, mouse, clone: 41–17[29]) was performed in the representative sections. CYP11B2 immunohistochemistry analysis was performed using the EnVision FLEX Kit (DAKO, Tokyo, Japan). The antigen-antibody complex was visualized by 3,3-diaminobenzidine (DAB) solution (1 mmol/L 3,3-diaminobenzidine) agents and counterstained with hematoxylin. All of the tissue sections used for immunohistochemistry was manually prepared by 1 experienced histotechnician at the Department of Pathology, Tohoku Graduate School of Medicine, exactly in the same fashion based on the protocol described in (Figure S1).

All immunostained tissue specimens were digitally scanned and captured using Image Scope AT2 for further analysis. We performed the first and second steps as those in the evaluation of H&E sections exactly in the same fashion and used the data of those H&E sections as the historical data because of the nature of the serial tissue sections. In corresponding to the first and second steps of DIA evaluation of H&E sections as above, CYP11B2 immunoreactivity was analyzed exclusively in cytoplasm (the area classified into cytoplasm in the parenchyme) by the gradients of brown color as a result of DAB reaction spectrum intensity. To further quantify the CYP11B2 immunoreactivity, we used the modified H-score system in this study.[29–31] The relative immunointensity of the gradient was evaluated as follows: negative as 0, weak (Yellow) as +1, moderate (Orange) as +2, and strong (Red) as +3, then calculated the *H* score of the unit area (mm^2) as Σ (Area of the individual gradients of the positive cells×Score 1+, 2+, 3+)/tumor area [the area of the cytoplasm]) using this DIA system (Figure 1B).[30–32]

As a confirmation of these evaluations, the parameters of these color spectrum and cell shape above were carefully reevaluated and concordant among 3 different observers (Ibuki Higashi, Y.S., Y.Y.) to minimize the interobserver variability and relative immunointensity of the cases was subsequently determined by DIA system.

Ultrastructural Evaluation Using DIA

Ultrastructural features of 2 *KCNJ5*-mutated APAs and 1 wild-type APA were further examined by transmission electron microscope. The pieces of specimen were harvested among the representative tumor areas and fixed with glutaraldehyde, following postfixation in osmium tetroxide, embedding epoxy, sliced at 80 nm, and staining with ura-nyl acetate and lead citrate. Fourteen representative tumor cells were selected among the grids of *KCNJ5*-mutated APAs and 15 tumor cells from wild-type APA as well. Area and number of lipid droplets as well as mitochondria were then quantitatively analyzed and calculated by DIA, using the software of Image-Scope v12.01.5027 (Leica, Aperio, Wetzlar, Germany). Representative illustration of quantitative ultra-structural analysis was summarized in Figure 1C.

Statistical Analysis

We analyzed the quantitative histopathological parameters as well as ultrastructural parameters between *KCNJ5*-mutated and wild-type APAs, using Mann-Whitney *U* test. The correlation between the proportion of the area of tumor cell subtypes and CYP11B2 immunoreactivity was also evaluated by Spearman test. *P* value <0.05 was considered significant. The software of JMP Pro ver.13.1.0 was used for statistical analysis.

Results

Clinicopathological characteristics of the cases examined and results of the statistical analysis of the digital quantitative his-topathological parameters were summarized in Figure 2A.

Quantitative Morphological Difference Between *KCNJ5*-Mutated and Wild-Type APAs

Parenchymal areas occupied 86.50% [82.43%–89.62%] in *KCNJ5*-mutated and 83.88% [77.99%–88.70%] in wild-type APAs, which was not significantly different between these 2 genotypes. However, the proportion of nuclear area was significantly higher in wild-type than in *KCNJ5*-mutated APAs *(KCNJ5* mutated: 6.83% [5.07%–8.77%] versus wild type: 13.82% [11.44%–18.99%], $P<0.0001$) and vice versa for the proportion of cytoplasm (79.47% [72.55%–82.84%] versus 69.13% [65.85%–73.32%]; $P=0.0027$). Average individual size of the nuclei was not significantly different, but average individual cell size in *KCNJ5*-mutated APAs was significantly larger than that of wild type (448.3 nm^2 [387.2–615.1 nm^2] versus 335.2 nm^2 [241.0–513.3 nm^2] $P=0.0158$), harboring significantly lower nuclear/cytoplasm ratio in *KCNJ5*-mutated APAs than in those of wild type (0.09 [0.06–0.12] versus 0.21 [0.100.43]; $P<0.0001$). Clear cell component was significantly more abundant in *KCNJ5*-mutated than in wild-type APAs (*KCNJ5* mutated: 71.76% [64.17%–80.42%] versus wild type: 53.00% [36.54%–65.13%]; $P=0.0041$) and vice versa in compact cell component *(KCNJ5* mutated: 28.25% [19.58%–35.84%] versus wild type: 47.00% [34.87%–63.46%]; $P=0.0041$). A significant positive correlation was detected between cell size and the proportion of clear cells in *KCNJ5* wild-type APA ($P=0.02$) but not in *KCNJ5*-mutated APA. However, there were no significant correlations between the tumor size and the proportion of clear cells regardless of the genotypes of APA. As illustrated in Figure 2B, in *KCNJ5*-mutated APAs, clear cell component was also significantly more abundant than

compact cell component (71.76% [64.17%–80.42%] versus 28.25% [19.58%–35.84%]; $P<0.0001$). However, the proportion of these clear and compact tumor cells were not significantly different between wild-type and mutated APAs (53.00% [36.54%–65.13%] versus 47.00% [34.87%–63.46%]; $P=0.3614$).

The percentage of adjacent ZG in adjacent adrenal cortex was not significantly different between these 2 genotypes *(KCNJ5* mutated: 13.27% [10.59%–16.73%] versus wild type: 9.43% [7.74%–15.26%]; $P=0.2427$), which indicated that the degree of paradoxical hyperplasia was not significantly different regardless of *KCNJ5* genotype.

Difference in CYP11B2 Immunoreactivity Between *KCNJ5*-Mutated and Wild-Type APAs

The status of CYP11B2 immunoreactivity (CYP11B2 *H* score/mm^2) was not significantly different between *KCNJ5*-mutated and wild-type APAs *(KCNJ5* mutated: 0.427 [0.280.47] versus wild type: 0.181 [0.12–0.53]; $P=0.0989$) as summarized in Figure 2A. In addition, CYP11B2 immunoreactivity was detected in some proportion of the area exclusively composed of each morphological cell subtype. The status of CYP11B2 immunoreactivity was not significantly different between clear and compact tumor cell components in both *KCNJ5*-mutated (clear: 0.162 [0.02–0.72] versus compact: 0.189 [0.03–0.79]; $P=0.6847$) and wild-type APAs (clear: 0.172 [0.02–1.39] versus compact: 0.125 [0.01–1.60]; $P=0.6281$).

Correlation Between the Proportion of Clear/Compact Cell Components and CYP11B2 Immunoreactivity in APAs From Different Genotypes

As illustrated in Figure 3, in all of the APA cases examined, CYP11B2 immunoreactivity (CYP11B2 *H* score/mm^2) was significantly correlated with the proportion of clear cell component in the tumor cytoplasmic area ($P=0.0021$; $\rho=0.50$) but inversely with the proportion of compact cells ($P=0.0021$; $\rho=-0.50$). However, no significant correlation was detected between the proportions of clear/compact tumor cell types and CYP11B2 immunoreactivity in each genotype of APAs, although CYP11B2 predominantly immunolocalized in the clear cell component in *KCNJ5*-mutated APAs ($P=0.07$; $\rho=0.43$).

Differences of Ultrastructural Features Between *KCNJ5*-Mutated and Wild-Type APAs

We also performed the quantitative ultrastructural analysis, that is, measurement of the area, size, and the number of lipid droplets as well as mitochondria in both genotypes of APAs to further clarify the potential intracellular biological activities of these morphological cell subtypes based on the development of intracellular organelles. As illustrated in Figure 4A, there were no significant differences in the average area of individual lipid droplets and the proportion of the area of lipid droplets against the cytoplasm between *KCNJ5*-mutated and wild-type APAs, but the number of lipid droplets per unit area was significantly more abundant in wild-type than in *KCNJ5*-mutated APA *(KCNJ5* mutated: 1.25E-04/nm^2 [1.07E-04/nm^2–1.56E-04/nm^2] versus wild type: 1.74E-04/nm^2 [1.54E-04/nm^2–2.32E-04/nm^2]; $P=0.0447$). The average area of individual mitochondria was significantly smaller in *KCNJ5*-mutated than in wild-type APA (*KCNJ5* mutated: 249.6 nm2 [201.6–267.0 nm^2] versus wild type: 366.6 nm^2 [329.3–406.9 nm^2]; $P=0.0002$). However, the number of mitochondria per unit area was significantly more abundant in *KCNJ5*-mutated

than in wild-type APA (*KCNJ5* mutated: 3.32E-04/nm^2 [2.41E-04/nm^2–4.00E-04/nm^2] versus wild type: 1.17E-04/nm^2 [7.59E-05/nm^2–2.49E-04/nm^2]; P=0.0035). In addition, as illustrated in Figure 4B, mitochondria in *KCNJ5*-mutated APA had more developed cristae than those in wild-type APA.

Discussion

To the best of our knowledge, this is the first detailed quantitative comparative histopathological study between *KCNJ5*-mutated and wild-type APAs. APA has been classically reported to be mainly composed of clear (zona fasciculata-like, lipid-rich cells) and compact tumor cells (ZG-like, spherical small cells). However, biological relevance of these terms or nomenclatures above has not been verified.[6,30,31] In addition, morphological differentiation between clear and compact cells in the studies above has been performed by eyeball analysis, which is usually reproducible by experienced endocrine pathologists, but results could be influenced by enormous interobserver variance and intratumoral heterogeneity. Therefore, in this study, we did firstly use an improved quantitative digital analytical method, using recently established HALO image software and precisely adjusted parameters of the color spectrum and cell shape, which could analyze in the widespread whole tumor areas to reflect the intratumoral heterogeneity with high reproducibility as well as to minimize the interobserver variability as much as possible.

Morphological Difference Between *KCNJ5*-Mutated and Wild-Type APA

KCNJ5-mutated APAs were reported to harbor relatively swelled nuclei,[33] but results of our present study did reveal that the average individual nuclear size was not significantly different between these genotypes of APAs, indicating that the size of the nuclei in *KCNJ5*-mutated APA was rather divergent, harboring the lower nuclear/cytoplasm ratio compared with wild-type APA. In addition, a significant inverse correlation was detected between nuclear/cytoplasm ratio and the proportion of clear tumor cell component in *KCNJ5*-mutated APAs (P=0.0319; ρ=−0.51). These results also indicated that the size of clear tumor cell was indeed larger than that of compact cells because of the enlargement of the lipid-rich cytoplasm, also consistent with relatively larger individual cell size of these tumors.

Clear cell component was reported to be generally predominant in *KCNJ5*-mutated APAs, and heteromorphic or relative predominance of compact tumor cells was more prominent in other APAs including wild type according to the previously published eyeball-based studies.[7,10,12,17,34,35] Results of our present study using DIA also revealed that clear tumor cells were significantly more predominant in *KCNJ5*-mutated APAs, whereas wild-type APAs harbored heteromorphic as in eyeball-based studied above.[7,10,12,17,34,35]

Clear tumor cells are considered to harbor more abundant lipid droplets possibly containing precursors of aldosterone in their enlarged cytoplasm. However, clear tumor cells have been considered biologically quiescent and compact cells relatively biologically active.[7–9] In addition, it is still controversial that *KCNJ5*-mutated APAs harbor clear tumor cell predominant morphological features or not. Therefore, we attempted to clarify the biological significance of these morphological phenotypes of APA cases based on CYP11B2

immunoreac-tivity and ultrastructural features to further explore whether these clear tumor cells, especially in *KCNJ5*-mutated APAs.

Difference of Biological Significance Between *KCNJ5*-Mutated and Wild-Type APAs Based on CYP11B2 Immunoreactivity

The possible discrepancy between results of previous studies and our present study could be because of the difference of methodology used in our present study, that is, CYP11B2 immunoreactivity was exclusively evaluated in the cytoplasm using DIA (Figure 1), after meticulous exclusion of mesenchyme and nuclear in parenchyme components of the specimens. In addition, the value of *H* score of clear tumor cells tended to become relatively low by eyeball-based evaluation primarily because of the masking of their abundant lipid-rich cytoplasm. Therefore, the value of relative immunointensity became rather condensed in our present DIA analysis. Of particular interest, CYP11B2 *H* score was not significantly different between clear and compact tumor cells in APAs with both genotypes, but CYP11B2 predominantly immunolocalized in clear tumor cells in *KCNJ5*-mutated APA. In contrast, CYP11B2 was immunolocalized both in clear and compact tumor cells in wild-type APAs. This finding did demonstrate that clear tumor cells were by no means biologically quiescent. However, it is also important to note that biological significance of these clear and compact tumor cell subtypes could not be evaluated only by CYP11B2 *H* score because of the nature of enlarged cytoplasm of clear tumor cells.

Biological Significance of Morphological Cell Subtypes in *KCNJ5*-Mutated and Wild-Type APAs

To further explore the intracellular biological activity of these clear tumor cells from different genotypes beyond the CYP11B2 immunoreactivity, we performed the quantitative ultrastructural analysis and quantified the area and number of lipid droplets as well as mitochondria. Results demonstrated that *KCNJ5*-mutated APAs had less lipid droplets but more abundant small-sized mitochondria with much more developed cristae, resulting in increased energy metabolism by enlargement of inner mitochondrial membrane (Figure 4B and 4C).[36,37] Therefore, these results did support the hypothesis of relatively biologically high active status of clear tumor cells present in *KCNJ5*-mutated APAs because they have not only abundant lipid droplets but also mitochondria, subsequently resulting in the biologically high active status of aldosterone biosynthesis.

Strengths and Limitation of the Study

A strength of our present study is that this quantitative histological analytical method could provide the detailed histological as well as ultrastructural features of APAs reflecting the intracellular biological activity. A limitation of our present study is, however, summarized as follows. First, the relatively small number of consecutive cases examined, entirely composed of Japanese cohorts. This could result in male predominance of *KCNJ5*-mutated APA cases in this study. However, histological difference was not detected between male and female patients examined in this study. Second, the status of medical therapy, such as the duration of antihypertensive agents and whether spironolactone was given or not, could possibly influence histological features of APAs. In our present study, none of the cases harbored spironolactone body but the changes according to the medications taken need to be evaluated

by further studies. Third, we could not exclude the possibility that the *KCNJ5*-mutated APA cases examined could simultaneously harbor other genetic mutations including *ATP1A1, ATP2B3, CACNA1D*, and *CTNNB1*.

Perspectives

Little is known about the intracellular biological significance of the morphologically identified APA tumor cell subtypes as clear and compact. Our present study could provide the novel insights into the histological features of APA tumor cell subtypes based on the biological spectrum. Clear tumor cells store intracellular lipid droplets of cholesterol ester as a precursor material of aldosterone biosynthesis and compact tumor cells represent the high density of intracytoplasmic organelles, such as mitochondria and smooth endoplasmic reticulum, where steroidogenic enzymes were located. Therefore, this equilibrium of aldosterone biosynthesis could possibly reveal that clear tumor cells are lipid-rich and possibly storage dominant status while compact tumor cells lipid-poor and possibly production dominant status (Figure 5B). However, further investigations are required to elucidate the precise biological features of these lipid droplets stored in the cytoplasm of clear tumor cells whether they represent the storage of cholesterol ester as precursors or the results of excessive status of aldosterone overproduction as well as the origin of the tumor cells.

Supplementary Material

Refer to Web version on PubMed Central for supplementary material.

Acknowledgments

Y. Yamazaki is supported by a scholarship from the Takeda Science Foundation. This work was supported by JSPS KAKENHI (Japan Society for the Promotion of Science; grant no. JP15H04711) and Health Labour Sciences Research Grant (No. H29-Nanji-Ippan-046). We also greatly appreciate Ibuki Higashi and Yuka Shishido for their excellent technical support for digital image analysis. Y. Yamazaki contributed the digital image analysis of hematoxylin and eosin (H&E), immunohistochemistry (IHC), and ultrastructural analysis. Y. Nakamura supported the histological evaluation. Y. Adachi took efforts to make sections examined for ultrastructural analysis. K. Ise took effort to prepare H&E sections as well as IHC sections. K. Omata, Y. Ono, Y. Tezuka, R. Morimoto, and F. Satoh contributed arrangement of the clinical data Tohoku University. Y. Shibahara contributed to arrange the adrenal sections from Yokohama Rosai Hospital. T. Kitamoto and T. Nakamura contributed arrangement of the clinical data from Yokohama Rosai Hospital. H. Sasano and F. Satoh supervised all of the present study.

References

1. Funder JW, Carey RM, Mantero F, Murad MH, Reincke M, Shibata H, Stowasser M, Young WF Jr. The management of primary aldosteronism: case detection, diagnosis, and treatment: an endocrine society clinical practice guideline. J Clin Endocrinol Metab. 2016;101:1889–1916. doi: 10.1210/jc.2015-4061 [PubMed: 26934393]
2. Mulatero P, Stowasser M, Loh KC, Fardella CE, Gordon RD, Mosso L, Gomez-Sanchez CE, Veglio F, Young WF Jr. Increased diagnosis of primary aldosteronism, including surgically correctable forms, in centers from five continents. J Clin Endocrinol Metab. 2004;89:1045–1050. doi: 10.1210/jc.2003-031337 [PubMed: 15001583]
3. Rossi GP, Bernini G, Caliumi C, et al.; PAPY Study Investigators. A prospective study of the prevalence of primary aldosteronism in 1,125 hypertensive patients. J Am Coll Cardiol. 2006;48:2293–2300. doi: 10.1016/j.jacc.2006.07.059 [PubMed: 17161262]

4. Nakamura Y, Felizola SJ, Satoh F, Konosu-Fukaya S, Sasano H. Dissecting the molecular pathways of primary aldosteronism. Pathol Int. 2014;64:482–489. doi: 10.1111/pin.12200 [PubMed: 25274410]
5. Nanba K, Chen AX, Omata K, Vinco M, Giordano TJ, Else T, Hammer GD, Tomlins SA, Rainey WE. Molecular heterogeneity in aldosterone-producing adenomas. J Clin Endocrinol Metab. 2016;101:999–1007. doi: 10.1210/jc.2015-3239 [PubMed: 26765578]
6. Azizan EAB, Lam BYH, Newhouse SJ, Zhou J, Kuc RE, Clarke J, Happerfield L, Marker A, Hoffman GJ, Brown MJ. Microarray, qPCR, and KCNJ5 sequencing of aldosterone-producing adenomas reveal differences in genotype and phenotype between zona glomerulosa- and zona fasciculata-like tumors. J Clin Endocrinol Metab. 2012; 97: 819–829. [PubMed: 22170727]
7. Monticone S, Castellano I, Versace K, Lucatello B, Veglio F, Gomez-Sanchez CE, Williams TA, Mulatero P. Immunohistochemical, genetic and clinical characterization of sporadic aldosterone-producing adenomas. Mol Cell Endocrinol. 2015;411:146–154. doi: 10.1016/j.mce.2015.04.022 [PubMed: 25958045]
8. Neville AM, O'Hare MJ. The Human Adrenal Cortex: Pathology and Biology-An Integrated Approach. Berlin, Germany: Springer-Verlag; 1982.
9. Tsuchiyama H, Kawai K, Harada T, Shigematsu K, Sugihara H. Functional pathology of aldosterone-producing adenoma. Acta Pathol Jpn. 1980;30:967–976. [PubMed: 6934686]
10. Choi M, Scholl UI, Yue P, et al. K+ channel mutations in adrenal aldosterone-producing adenomas and hereditary hypertension. Science. 2011;331:768–772. doi: 10.1126/science.1198785 [PubMed: 21311022]
11. Beuschlein F, Boulkroun S, Osswald A, et al. Somatic mutations in ATP1A1 and ATP2B3 lead to aldosterone-producing adenomas and secondary hypertension. Nat Genet. 2013;45:440–444, 444e1. doi: 10.1038/ng.2550 [PubMed: 23416519]
12. Azizan EA, Poulsen H, Tuluc P, et al. Somatic mutations in ATP1A1 and CACNA1D underlie a common subtype of adrenal hypertension. Nat Genet. 2013;45:1055–1060. doi: 10.1038/ng.2716 [PubMed: 23913004]
13. Berthon A, Drelon C, Ragazzon B, et al. WNT/β-catenin signalling is activated in aldosterone-producing adenomas and controls aldosterone production. Hum Mol Genet. 2014;23:889–905. doi: 10.1093/hmg/ddt484 [PubMed: 24087794]
14. Taguchi R, Yamada M, Nakajima Y, Satoh T, Hashimoto K, Shibusawa N, Ozawa A, Okada S, Rokutanda N, Takata D, Koibuchi Y, Horiguchi J, Oyama T, Takeyoshi I, Mori M. Expression and mutations of KCNJ5 mRNA in Japanese patients with aldosterone-producing adenomas. J Clin Endocrinol Metab. 2012;97:1311–1319. doi: 10.1210/jc.2011-2885 [PubMed: 22278422]
15. Williams TA, Peitzsch M, Dietz AS, Dekkers T, Bidlingmaier M, Riester A, Treitl M, Rhayem Y, Beuschlein F, Lenders JW, Deinum J, Eisenhofer G, Reincke M. Genotype-specific steroid profiles associated with aldosterone-producing adenomas. Hypertension. 2016;67:139–145. doi: 10.1161/HYPERTENSIONAHA.115.06186 [PubMed: 26573708]
16. Arnesen T, Glomnes N, Strømsøy S, Knappskog S, Heie A, Akslen LA, Grytaas M, Varhaug JE, Gimm O, Brauckhoff M. Outcome after surgery for primary hyperaldosteronism may depend on KCNJ5 tumor mutation status: a population-based study from Western Norway. Langenbecks Arch Surg. 2013;398:869–874. doi: 10.1007/s00423-013-1093-2 [PubMed: 23778974]
17. Kitamoto T, Suematsu S, Yamazaki Y, Nakamura Y, Sasano H, Matsuzawa Y, Saito J, Omura M, Nishikawa T. Clinical and steroidogenic characteristics of aldosterone-producing adenomas with ATPase or CACNA1D gene mutations. J Clin Endocrinol Metab. 2016;101:494–503. doi: 10.1210/jc.2015-3284 [PubMed: 26606680]
18. Gudlaugsson E, Skaland I, Janssen EA, Smaaland R, Shao Z, Malpica A, Voorhorst F, Baak JP. Comparison of the effect of different techniques for measurement of Ki67 proliferation on reproducibility and prognosis prediction accuracy in breast cancer. Histopathology. 2012;61:1134–1144. doi: 10.1111/j.1365-2559.2012.04329.x [PubMed: 22963617]
19. Koopman T, de Bock GH, Buikema HJ, Smits MM, Louwen M, Hage M, Imholz ALT, van der Vegt B. Digital image analysis of HER2 immuno-histochemistry in gastric- and oesophageal adenocarcinoma: a validation study on biopsies and surgical specimens. Histopathology. 2018;72:191–200. doi: 10.1111/his.13322 [PubMed: 28746978]

20. Jones RL, Salter J, A'Hern R, Nerurkar A, Parton M, Reis-Filho JS, Smith IE, Dowsett M. Relationship between oestrogen receptor status and proliferation in predicting response and long-term outcome to neoadjuvant chemotherapy for breast cancer. Breast Cancer Res Treat. 2010;119:315–323. doi: 10.1007/s10549-009-0329-x [PubMed: 19247830]
21. Hagiya AS, Etman A, Siddiqi IN, Cen S, Matcuk GR Jr, Brynes RK, Salama ME. Digital image analysis agrees with visual estimates of adult bone marrow trephine biopsy cellularity. Int J Lab Hematol. 2018;40:209–214. doi: 10.1111/ijlh.12768 [PubMed: 29222848]
22. Ono Y, Nakamura Y, Maekawa T, Felizola SJ, Morimoto R, Iwakura Y, Kudo M, Seiji K, Takase K, Arai Y, Gomez-Sanchez CE, Ito S, Sasano H, Satoh F. Different expression of 11β-hydroxylase and aldosterone synthase between aldosterone-producing microadenomas and macroadenomas. Hypertension. 2014;64:438–444. doi: 10.1161/HYPERTENSIONAHA.113.02944 [PubMed: 24842915]
23. Kitamoto T, Omura M, Suematsu S, Saito J, Nishikawa T. KCNJ5 mutation as a predictor for resolution of hypertension after surgical treatment of aldosterone-producing adenoma. J Hypertens. 2018;36:619–627. doi: 10.1097/HJH.0000000000001578 [PubMed: 29016532]
24. Weiss LM. Comparative histologic study of 43 metastasizing and nonmetastasizing adrenocortical tumors. Am J Surg Pathol. 1984;8:163–169. [PubMed: 6703192]
25. Gioco F, Seccia TM, Gomez-Sanchez EP, Rossi GP, Gomez-Sanchez CE. Adrenal histopathology in primary aldosteronism: is it time for a change? Hypertension. 2015;66:724–730. doi: 10.1161/HYPERTENSIONAHA.115.05873 [PubMed: 26238443]
26. Felizola SJ, Nakamura Y, Ono Y, Kitamura K, Kikuchi K, Onodera Y, Ise K, Takase K, Sugawara A, Hattangady N, Rainey WE, Satoh F, Sasano H. PCP4: a regulator of aldosterone synthesis in human adrenocortical tissues. J Mol Endocrinol. 2014;52:159–167. doi: 10.1530/JME-13-0248 [PubMed: 24403568]
27. Azizan EA, Brown MJ. Novel genetic determinants of adrenal aldosterone regulation. Curr Opin Endocrinol Diabetes Obes. 2016;23:209–217. doi: 10.1097/MED.0000000000000255 [PubMed: 26992195]
28. Sasano H, Okamoto M, Sasano N. Immunohistochemical study of cytochrome P-450 11 beta-hydroxylase in human adrenal cortex with mineralo- and glucocorticoid excess. Virchows Arch A Pathol Anat Histopathol. 1988;413:313–318. [PubMed: 3140475]
29. Gomez-Sanchez CE, Qi X, Velarde-Miranda C, Plonczynski MW, Parker CR, Rainey W, Satoh F, Maekawa T, Nakamura Y, Sasano H, Gomez-Sanchez EP. Development of monoclonal antibodies against human CYP11B1 and CYP11B2. Mol Cell Endocrinol. 2014;383:111–117. doi: 10.1016/j.mce.2013.11.022 [PubMed: 24325867]
30. Yamazaki Y, Nakamura Y, Omata K, Ise K, Tezuka Y, Ono Y, Morimoto R, Nozawa Y, Gomez-Sanchez CE, Tomlins SA, Rainey WE, Ito S, Satoh F, Sasano H. Histopathological classification of cross-sectional image-negative hyperaldosteronism. J Clin Endocrinol Metab. 2017;102:1182–1192. doi: 10.1210/jc.2016-2986 [PubMed: 28388725]
31. Konosu-Fukaya S, Nakamura Y, Satoh F, et al. 3β-Hydroxysteroid dehydrogenase isoforms in human aldosterone-producing adenoma. Mol Cell Endocrinol. 2015;408:205–212. doi: 10.1016/j.mce.2014.10.008 [PubMed: 25458695]
32. McCarty KS Jr, Miller LS, Cox EB, Konrath J, McCarty KS Sr. Estrogen receptor analyses. Correlation of biochemical and immunohistochemical methods using monoclonal antireceptor antibodies. Arch Pathol Lab Med. 1985;109:716–721. [PubMed: 3893381]
33. Tan GC, Negro G, Pinggera A, et al. Aldosterone-producing adenomas: histopathology-genotype correlation and identification of a novel CACNA1D mutation. Hypertension. 2017;70:129–136. doi: 10.1161/HYPERTENSIONAHA.117.09057 [PubMed: 28584016]
34. Scholl UI, Healy JM, Thiel A, et al. Novel somatic mutations in primary hyperaldosteronism are related to the clinical, radiological and pathological phenotype. Clin Endocrinol (Oxf). 2015;83:779–789. doi: 10.1111/cen.12873 [PubMed: 26252618]
35. Fernandes-Rosa FL, Williams TA, Riester A, et al. Genetic spectrum and clinical correlates of somatic mutations in aldosterone-producing adenoma. Hypertension. 2014;64:354–361. doi: 10.1161/HYPERTENSIONAHA.114.03419 [PubMed: 24866132]

36. Papadopoulos V, Miller WL. Role of mitochondria in steroidogenesis. Best Pract Res Clin Endocrinol Metab. 2012;26:771–790. doi: 10.1016/j.beem.2012.05.002 [PubMed: 23168279]

37. Chien Y, Rosal K, Chung BC. Function of CYP11A1 in the mitochondria. Mol Cell Endocrinol. 2017;441:55–61. doi: 10.1016/j.mce.2016.10.030 [PubMed: 27815210]

Novelty and Significance

What Is New?

- Digital image quantitative histological analysis could firstly characterize the histology of *KCNJ5*-mutated aldosterone-producing adenoma as enlarged lipid-rich tumor cells containing abundant small-sized mitochondria with well-developed cristae harboring under the storage dominant biologically high active status.

What Is Relevant?

- Characteristic quantitative histological features could help to clarify the primary aldosteronism pathophysiology in terms of intracellular equilibrating conditions of aldosterone biosynthesis.

Summary

Our present study did provide novel insights into the aldosterone-producing adenoma tumor cell subtypes based on the intracellular hormonal activity beyond CYP11B2 immunoreactivity.

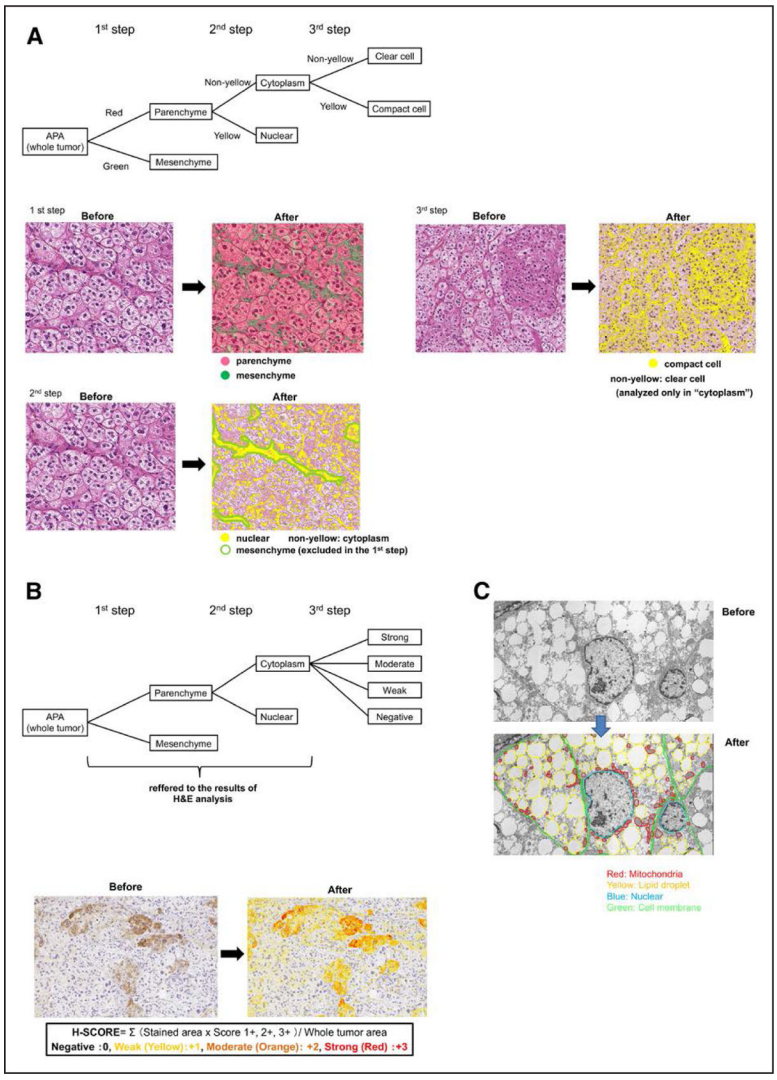

Figure 1.

Representative illustrations of the newly developed quantitative histological digital image analysis (DIA). **A**, Representative illustrations of the detailed process of quantitative morphological evaluation. In the first step, we circumscribed the whole tumor area as the annotation analyzed area. The whole tumor area was initially classified into parenchyme and mesenchyme based on the histological architectural patterns, including the cell shape and color spectrums. The area composed of clear or compact tumor cells constituting the alveolar architecture was tentatively classified as parenchyme. The area composed of vascular structures and collagen fibers with abundant spindle-shaped fibroblasts tentatively classified as mesenchyme. Histological architectural patterns of these 2 components were distinctively distinguishable from each other. Parenchyme was tentatively colored in red and mesenchyme in green. In the second step, we extracted parenchyme for subsequent classification into nuclear and cytoplasm. Mesenchyme has been already excluded in the first step. This second classification was based on the color spectrums as nuclear: purple (hematoxylin), cytoplasm: nonpurple. Nuclear was marked as yellow recognized by DIA as the purple color spectrum of hematoxylin staining. In the third step, after nuclear was

excluded in the second step, cytoplasm was finally extracted, corresponding to the area classified into cytoplasm in the parenchyme. Finally, cytoplasm was further classified into clear cells and compact cells based on the gradients of the eosinophilic color spectrum. **B**, Representative illustrations of the detailed process of digital image immunohistochemistry (IHC) evaluation As mentioned in **A**, we started from the third step corresponding to hematoxylin and eosin (H&E)-stained tissue sections analytical protocol by DIA because of the same situation in first and second steps. We used the historical data from the H&E-stained tissue sections analysis after the second step because of the nature of serial tissue sections. CYP11B2 immunoreactivity was analyzed only in cytoplasm by the gradients of brownish color (3,3-diaminobenzidine, DAB) spectrum intensity. H-score analytical quantitative method was applied to DIA system. The relative immunointensity of the gradient was evaluated as follows: Negative as 0, Weak (Yellow) as +1, Moderate (Orange) as +2, and Strong (Red) as +3, then calculated the *H* score of the unit area along with the formula shown in the figure. **C**, Representative illustrations of the quantitative ultrastructural analysis. After we took the representative pictures and integrated the images, we circumscribed the each intracellular structure of nuclear (blue), lipid droplets (yellow), and mitochondria (red). The precise area of each structure was calculated by the software of Image-Scope v12.01.5027 (Leica, Aperio, Wetzlar, Germany). APA indicates aldosterone-producing adenoma.

A

		KCNJ5 mutated (n=18)	Wild type (n=17)	*P value* [Value: Q2 (Q1-Q3)]
Clinical characteristics	Age	47 (43～59)	54 (49～60)	
	Gender	F: 6, M: 12	F: 12, M: 5	
	Size [mm]	15 (13～20)	15 (11～16)	
	SBP [mmHg]	152 (141～157)	138 (126～155)	
	DBP [mmHg]	93 (82～99)	86 (73～99)	
	Serum K (including supplementation) [mmol/L]	3.8 (3.5～4.2)	3.3 (2.8～3.5)	
	PRA [ng/ml/hr]*	0.15 (0.10～0.45)	0.20 (0.20～0.30)	
	PAC* [ng/dl]	24.15 (21.13～38.70)	31.20 (23.20～50.50)	
	ARR*	205.0 (38.52～247.8)	159 (85.80～252.0)	
	Captopril loading ARR after 90 min*	156.0 (53.83～306.0)	201.4 (84.90～282.8)	
Morphological DIA	**Parenchyme [%]**	86.50 (82.43～89.62)	83.88 (77.99～88.70)	*0.3221*
	Mesenchyme [%]	13.50 (10.38～17.58)	16.12 (11.30～22.01)	*0.3221*
	Nuclear [%]	6.83 (5.07～8.77)	13.82 (11.44～18.99)	***<.0001****
	Cytoplasm [%]	79.47 (72.55～82.84)	69.13 (65.85～73.32)	***0.0027****
	N/C ratio	0.09 (0.06～0.12)	0.21 (0.16～0.31)	***<.0001****
	Nuclear size [μm^2]	46.84 (36.52～60.00)	53.46 (49.08～79.14)	*0.1497*
	Cell size [μm^2]	448.3 (387.2～615.1)	335.2 (241.0～513.3)	***0.0158****
	Clear cell component / Cytoplasm[%]	71.76 (64.17～80.42)	53.00 (36.54～65.13)	***0.0041****
	Compact cell component / Cytoplasm [%]	28.25 (19.58～35.84)	47.00 (34.87～63.46)	***0.0041****
	CYP11B2 positive area / Cytoplasm [%]	30.70 (21.07～34.61)	14.02 (9.43～36.59)	*0.1058*
	CYP11B2 H-score (Cytoplasm) [/mm^2]	0.427 (0.28～0.47)	0.181(0.12～0.53)	*0.0989*
	Area of adjacent ZG /cortex [%]	13.27 (10.59～16.73)	9.43 (7.74～15.26)	*0.2427*

B

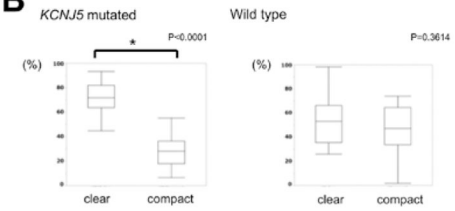

Figure 2.

Clinicopathological characteristics of aldosterone-producing adenoma (APA) cases examined in this study. Value: Q2 (Q1–Q3). Among 35 APA cases, 18 cases harboring *KCNJ5* mutation from Tohoku University Hospital and 17 cases harboring wild type from Yokohama Rosai Hospital. (*): *P* values of comparison of clinical laboratory data were not provided because these 2 groups were used from different institutions. **A**, Results of quantitative morphological evaluation of *KCNJ5*-mutated and wild-type APAs. Morphological difference between *KCNJ5*-mutated and wild-type APAs revealed that *KCNJ5*-mutated APA was characterized by the morphometry of low nuclear/cytoplasm (N/C) ratio with enlarged cytoplasm and clear cell predominancy. The values of the proportion of parenchyme, mesenchyme, nuclear, and cytoplasm were calculated against the whole tumor area and those of the proportion of clear cell, compact cell, CYP11B2 positive area, and CYP11B2 *H* score against the cytoplasm in the parenchyme. **B**, Comparison of the proportion of morphological cell components in APA of each genotype. Clear cell component was significantly more abundant than compact 1 in *KCNJ5*-mutated APAs (clear: 71.76% [64.17%–80.42%] vs compact: 28.25% [19.58%–35.84%]; $P<0.0001$), whereas wild-type APAs harbored heteromorphic or relatively higher proportion of compact tumor cell components than *KCNJ5*-mutated APAs (clear: 53.00% [36.54%–65.13%] vs compact: 47.00% [34.87%–63.46%]; $P=0.3614$). ARR indicates PAC/PRA (aldosterone/renin ratio); DBP, diastolic blood pressure; DIA, digital image analysis; PAC, plasma aldosterone concentration; PRA, plasma renin activity; SBP, systolic blood pressure; and ZG, zona glomerulosa.

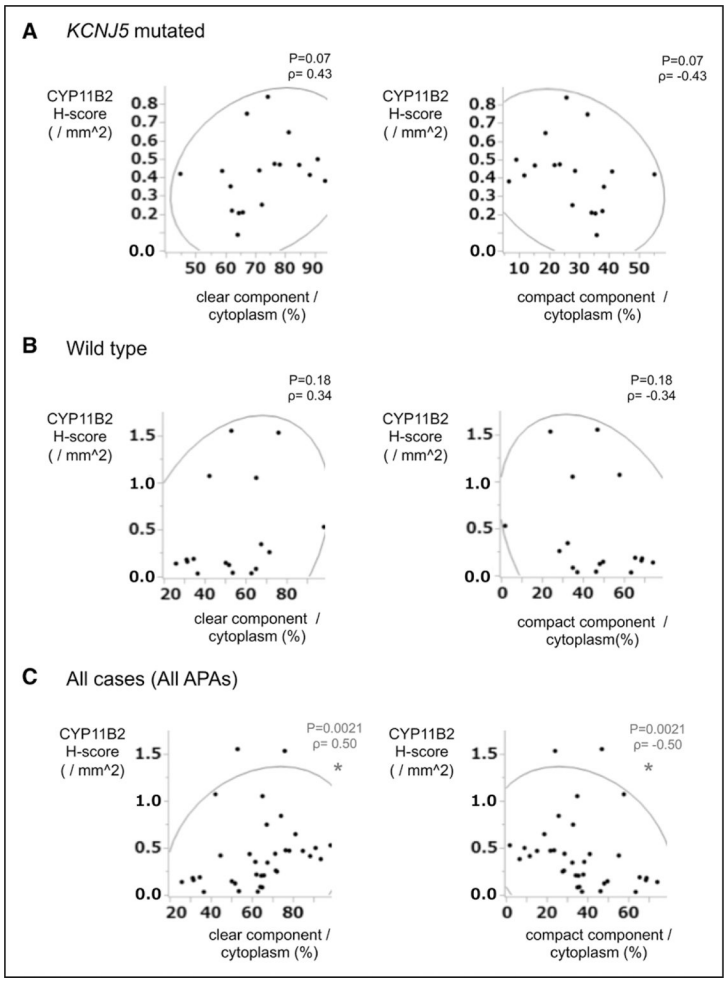

Figure 3.

Correlation between the proportion of clear/compact tumor cell components and CYP11B2 immunoreactivity in each genotype by digital image analysis (DIA). **A**, The proportion of clear/compact cell component tended to be associated with CYP11B2 immunoreactivity (CYP11B2 *H* score) in *KCNJ5*-mutated APAs (vs clear: P=0.07, ρ=0.43, vs compact: P=0.07, ρ=0.43) although not reaching statistical significance. **B**, There were no significant correlations between the proportions of compact/clear tumor cell types and CYP11B2 immunoreactivity in aldosterone-producing adenomas (APAs) harboring wild type. **C**, In all the cases of APAs, there was a significantly positive correlation between the proportion of clear tumor cell component and CYP11B2 immunoreactivity (P=0.0021, ρ=0.50) as well as inverse correlation between the proportion of compact tumor cells and CYP11B2 immunoreactivity (P=0.0021, ρ=−0.50).

A

[Value: Q2 (Q1-Q3)]

		KCNJ5 mutated (n=14 cells)	Wild type (n=15 cells)	*P value*
Ultrastructual DIA	Av. area of lipid [nm^2]	3096.2 (2352.2～3913.3)	2462.9 (1927.4～2876.9)	*0.0887*
	No. of lipid [/nm^2]	1.25E-04 (1.07E-04～1.56E-04)	1.74E-04 (1.54E-04～2.32E-04)	***0.0447****
	Area of lipid / cytoplasm [%]	38.1 (34.1～42.3)	55.8 (31.2～60.2)	*0.1378*
	Av. area of mitochondria [nm^2]	249.6 (201.6～267.0)	366.6 (329.3～406.9)	***0.0002****
	No. of mitochondria [/nm^2]	3.32E-04 (2.41E-04～4.00E-04)	1.17E-04 (7.59E-05～2.49E-04)	***0.0035****
	Area of mitochondria / cytoplasm [%]	7.97 (5.00～9.08)	4.40 (3.11～7.97)	*0.0887*

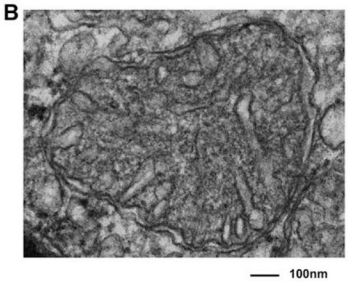

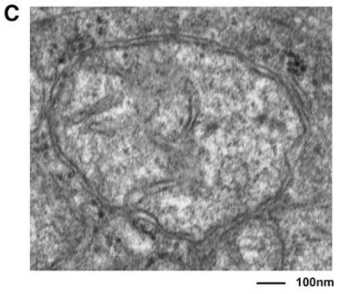

Figure 4.

Quantitative ultrastructual analysis in *KCNJ5*-mutated and wild-type aldosterone-producing adenoma (APA). **A**, Results of quantitative ultrastructural analysis in *KCNJ5*-mutated cells and wild-type tumor cells. Fourteen tumor cells from 2 *KCNJ5*-mutated APA cases (CYP11B2 *H* score: 0.57/mm^2 and 0.80/mm^2) and 15 tumor cells from 1 wild-type APA case (CYP11B2 *H* score: 0.18/mm^2) were selected among the different grids. Grids of both genotypes of APAs were predominantly composed of clear tumor cells. Value: Q2 (Q1–Q3). **B, C**, Representative ultrastructural images of mitochondria in *KCNJ5*-mutated (**B**) and wild-type APAs (**C**). Mitochondria in *KCNJ5*-mutated cells were small but had well-developed cristae, in contrast, those in wild-type cells were relatively large with their cristae not so well developed as those of *KCNJ5*-mutated cells. Av. indicates average; DIA, digital image analysis; lipid/cytoplasm, proportion of the area of lipid droplets against the area of cytoplasm; and mitochondria/cytoplasm, proportion of the area of mitochondria against the area of cytoplasm.

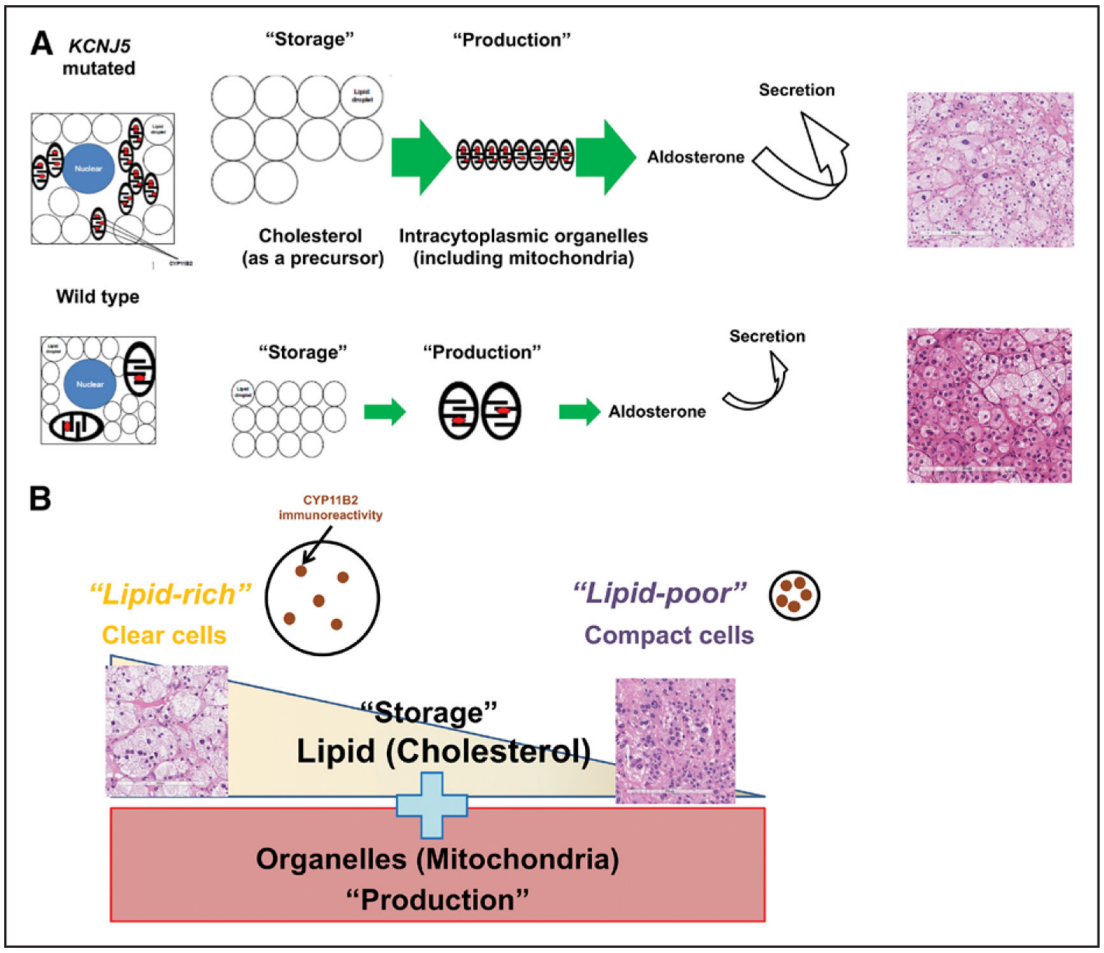

Figure 5.

Hypothetical biological status of cell subtypes in aldosterone-producing adenoma (APA). **A**, Intracellular biological significance of clear tumor cells in *KCNJ5*-mutated APAs and wild type. Clear tumor cells observed in *KCNJ5*-mutated APAs had not only abundant lipid droplets as well as abundant mitochondria with well-developed cristae, resulting in the extremely high biological active status of aldosterone biosynthesis. However, clear tumor cells observed in wild-type APAs had more abundant lipid droplets, but the number of mitochondria was not so much as those observed in *KCNJ5*-mutated APA, resulting in relatively high but lower biological active status of aldosterone biosynthesis than *KCNJ5*-mutated APA. **B**, Histopathological classification of tumor cell subtypes in APA based on the intracellular biological significance beyond CYP11B2 immunoreactivity. Clear tumor cells had not only abundant lipid droplets in their enlarged cytoplasm but also intracytoplasmic organelles including mitochondria. The presence of these abundant intracellular lipid droplets could possibly indicate the relatively large amount of cholesterol provided as precursor materials of aldosterone. However, these cells also had relatively high density of intracytoplasmic mitochondria containing CYP11B2, which could convert the precursors into aldosterone. Considering the status of intracellular equilibrium between storage and production in the process of aldosterone biosynthesis, abundant intracellular storage of lipid droplets rather than abundant organelles represented the features of clear

tumor cells. Therefore, clear tumor cells were lipid-rich harboring relatively storage dominant cells, resulting in biologically high activity of aldosterone biosynthesis, especially in *KCNJ5*-mutated APAs. However, it is also important to note that CYP11B2 immunoreactivity (CYP11B2 *H* score) tends to become lower because of the nature of enlarged cytoplasm of the clear tumor cells. On the other hand, compact tumor cells were lipid-poor harboring relatively production dominant cells. In *KCNJ5*-mutated APAs, aldosterone production in compact tumor cells was considered to be low based on CYP11B2 immunolocalization, which possibly reflected the status of exhaustion of lipid droplets.